Depth vs. Age

- **Parsons and Sclater, 1977**

  careful analysis, basically correct answer

- **Stein and Stein, 1992**

  careless analysis, basically wrong answer, Lake Wobegon Effect

- **Doin and Fleitout, 1996**

  different interpretation for flattening

- **Hillier and Watts, 2005**

  more careful depth versus age, better answer – same as P&S 1977

oceanic lithosphere dominates mantle convection

largest surface area

greatest temperature drop across TBL = largest density contrast

> 1/2 of heat escapes in young oceanic lithosphere

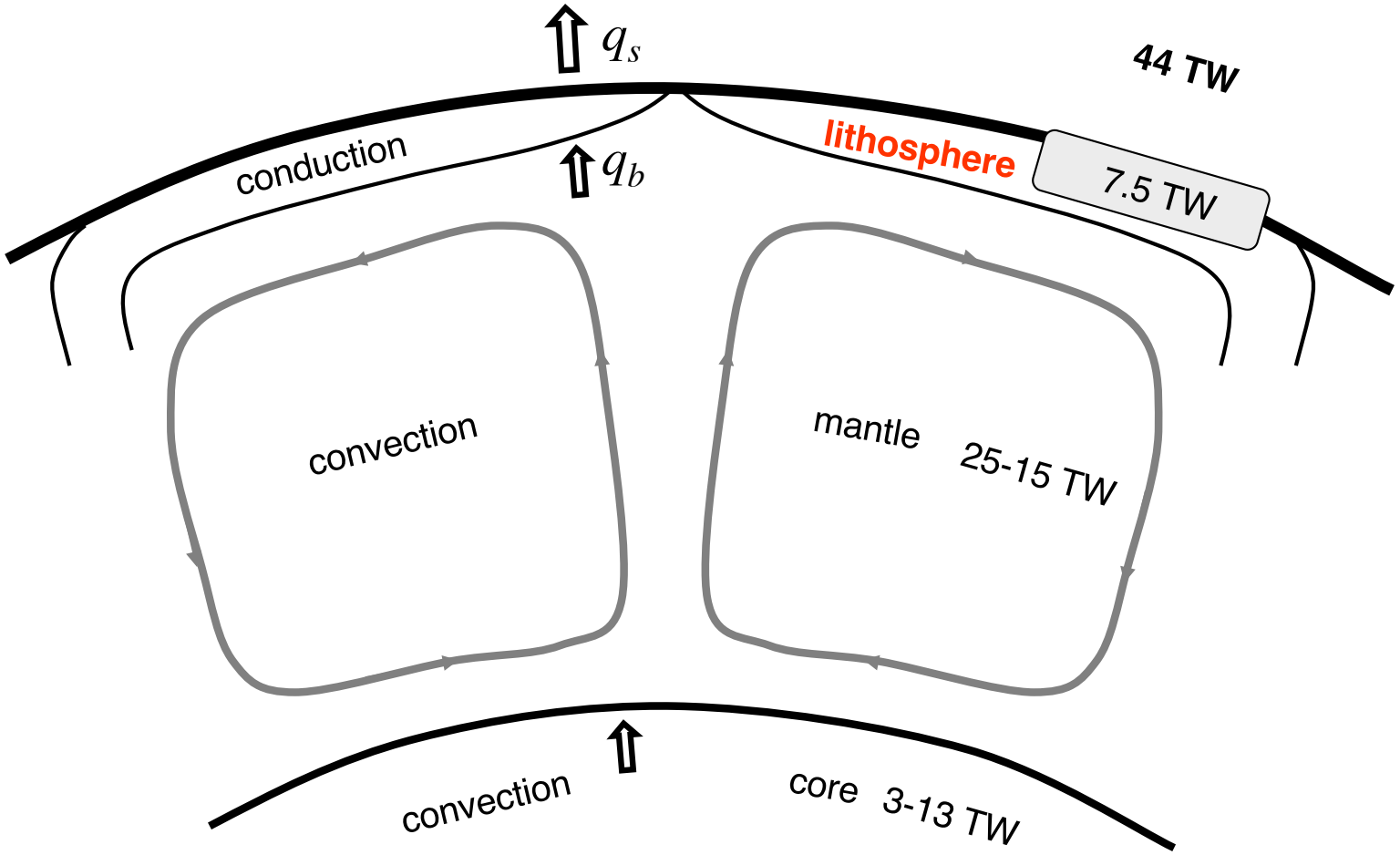

isostatic compensation

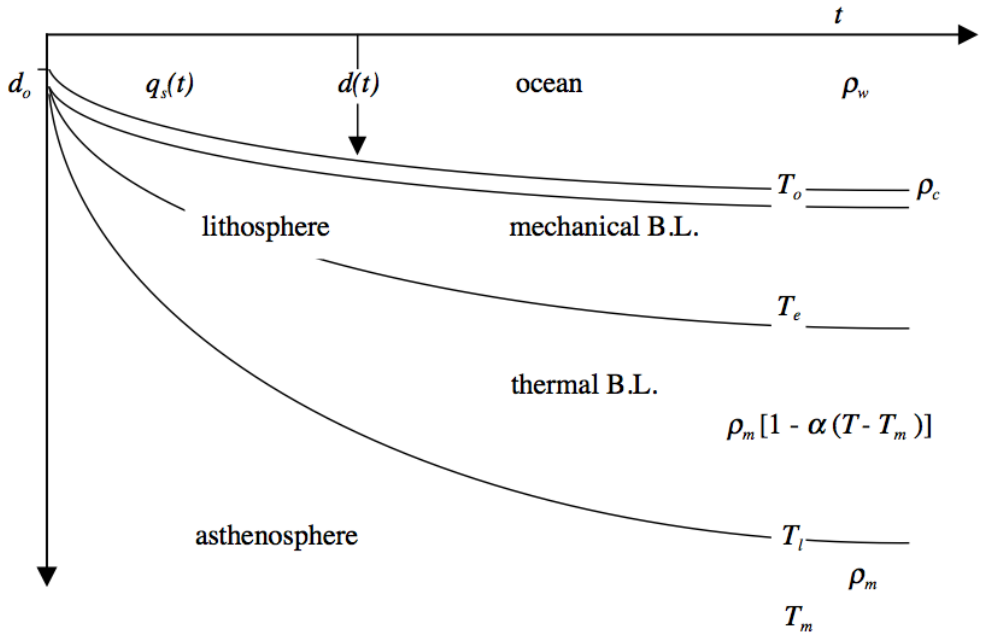

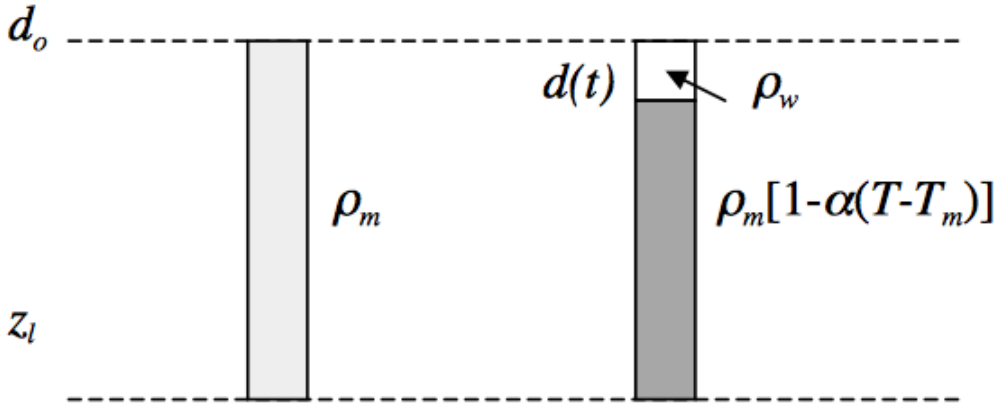

$$g\int_o^{z_l}\rho_m dz = g\int_o^{d}\rho_w dz + g\int_d^{z_l}\rho_m\left[1-\alpha\left(T-T_m\right)\right]dz$$

half space cooling

$$T(z,t) = T_o + (T_m - T_o)\,erf\left(\frac{z}{2\sqrt{\kappa t}}\right)$$

$$q(t) = \frac{k(T_m - T_o)}{\sqrt{\pi \kappa t}}$$

$$d(t) = d_o + \frac{2\alpha\rho_m (T_m - T_o)}{(\rho_m - \rho_w)}\sqrt{\frac{\kappa t}{\pi}}$$

plate cooling cooling

$$T(z,t) = T_o + (T_m - T_o)\left[\frac{z}{L} + \sum_{n=1}^{\infty}\frac{2}{\pi}\exp\left(\frac{-n^2\pi^2\kappa t}{L^2}\right)\sin\left(\frac{n\pi z}{L}\right)\right]$$

$$q(t) = \frac{k(T_m - T_o)}{L}\left[1 + 2\sum_{n=1}^{\infty}\exp\left(\frac{-n^2\pi^2\kappa t}{L^2}\right)\right]$$

$$d(t) = d_o + \frac{\alpha\rho_m (T_m - T_o)L}{2(\rho_m - \rho_w)}\left[1 - \frac{2}{\pi^2}\sum_{n=0}^{\infty}\frac{1}{(1+2n)^2}\exp\left(\frac{-(1+2n)^2\pi^2\kappa t}{L^2}\right)\right]$$

Parameter	Definition	Value
T_o	surface temperature	0˚C
T_m	mantle temperature	1300˚-1500˚C
κ	thermal diffusivity	8 x 10^{-7} m^2 s^{-1}
k	thermal conductivity	3.3 W m^{-1} C^{-1}
α	thermal expansion coefficient	3.1-4.2 x 10^{-5} C^{-1}
ρ_w	seawater density	1025 kg m^{-3}
ρ_m	mantle density	3300 kg m^{-3}
d_o	ridge axis depth	2500-3000 m
L	plate thickness	95-130 km, ∞

AN ANALYSIS OF THE VARIATION OF OCEAN FLOOR BATHYMETRY AND HEAT FLOW WITH AGE

Barry Parsons and John G. Sclater

Department of Earth and Planetary Sciences, Massachusetts Institute of Technology
Cambridge, Massachusetts 02139

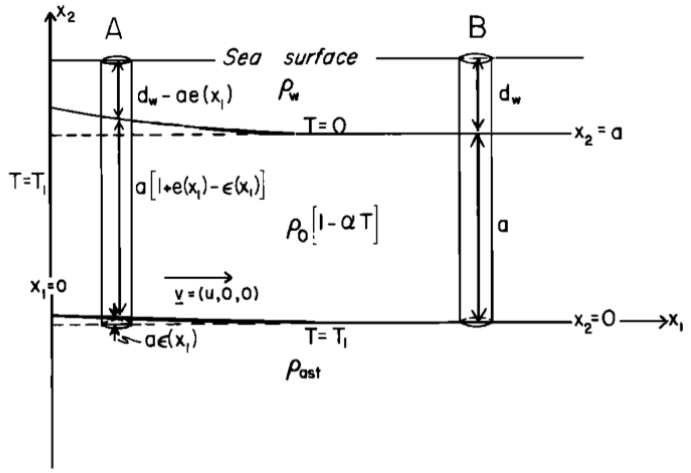

Fig. 1. Sketch showing the geometry and boundary conditions of the plate model and the method of calculating the elevation. Columns A and B of equal cross-sectional area must have equal masses above a common level $x_2 = 0$. This gives

$$\rho_w d_w + \int_0^a \rho_o[1 - \alpha T(\infty, x_2)]\, dx_2 = \rho_w[d - ae(x_1)] + \int_{a\varepsilon(x_1)}^{a[1+\rho(x_1)]} \rho_o[1 - \alpha T(x_1, x_2)]\, dx_2 + \rho_{ast}\, a\varepsilon(x_1)$$

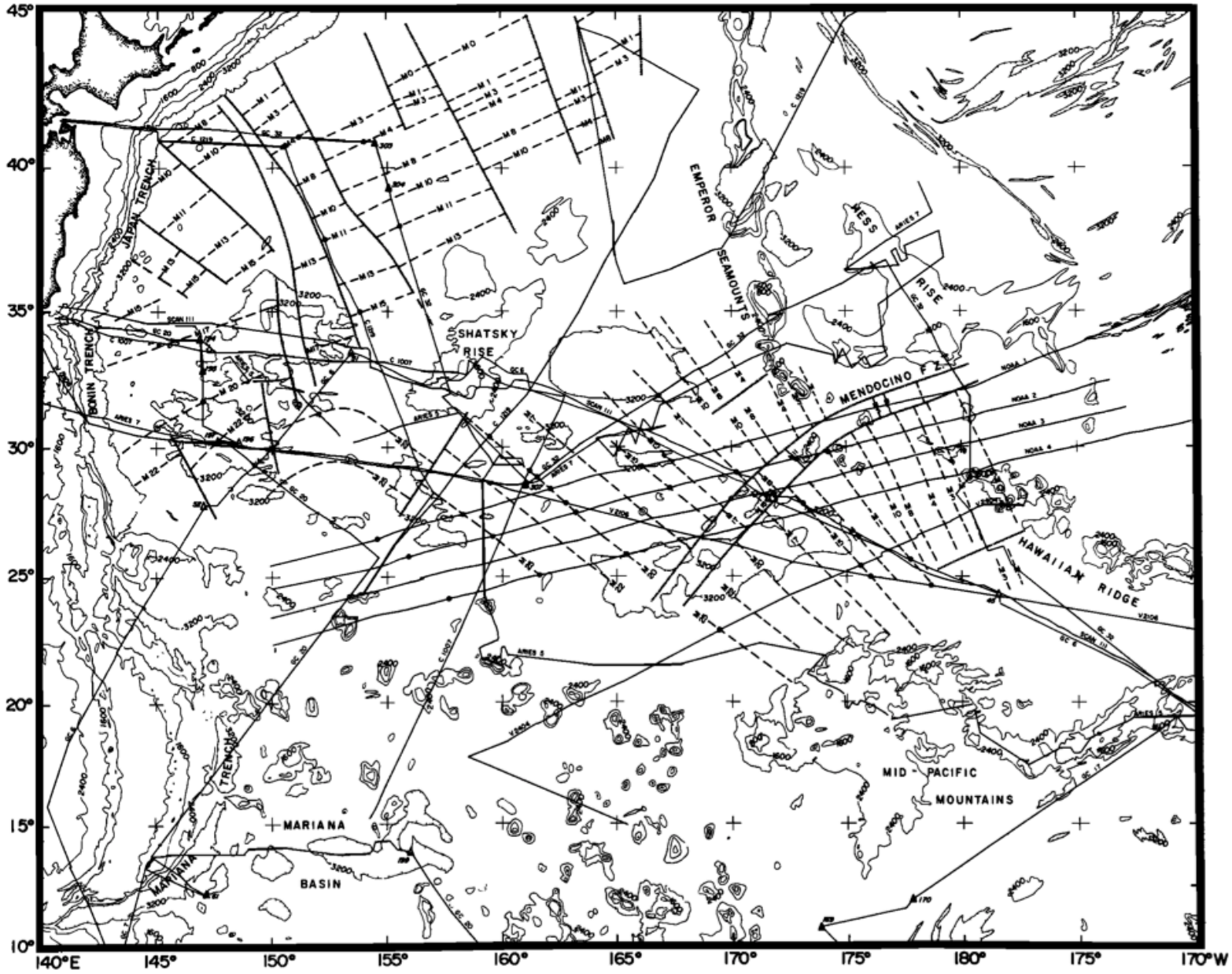

Fig. 6. Mesozoic magnetic lineations, ship tracks with seismic reflection profiles, bathymetric contours, and DSDP sites in the northwestern Pacific Ocean. The lineations are based on Hilde et al. [1976], and Larson and Hilde [1975]. The bathymetric contours are from Chase et al. [1970] and are in uncorrected fathoms. Open triangles denote DSDP sites, listed in Table 2; solid triangles indicate that basement was reached. Solid circles denote the location of depth measurements.

TABLE 2. Depth and Sediment Thickness at Joides Drill Holes in the Northwestern Pacific with Magnetic Anomaly or Biostratigraphic Ages

Site	Latitude	Longitude	Depth, m	Sediment Thickness Estimated From Profiles*, m	Penetration, m	Sediment Correction*, m	Corrected Depth, m	Biostratigraphic Zone or Comments	Magnetic Anomaly†	Age†, m.y.B.P.	Comments on Seismic Record
45	24°15.9'N	178°30.5'W	5508	600	105	420	5928	...	M3-4	115	Not clear
46	27°53.8'N	171°26.3'E	5769	400	9	280	6049	Close to Fracture Zone	M15	133	Clear
51	33°28.5'N	153°24.3'E	5981	400	132	280	6261	Edge of Shatsky Rise, Topographic Relief Large	M17	137	Clear
52	27°46.3'N	147°07.8'E	5744	(300)	69	210	5954	...	M24-25	152	Basement estimate given in site report
61‡	12°05.0'N	147°03.7'E	5570	135	98#	95	5665	On Trench Outer Rise	...	...	Clear, probably 30 m more sediment to basement
66‡	2°23.6'N	166°7.3'W	5293	235	192#	134	5427	Turonian or Cenomanian, Pronounced Basement High	...	87-100	Clear
164	13°12.1'N	161°31.0W	5499	300	264#	185	5684	Barremian-Albian	...	100-118	Clear
165	8°10.7'N	164°51.6W	5053	500	470#	329	5382	>Campanian, Edge of Line Islands	...	75-85	Clear
166‡	3°45.7'N	175°04.8'W	4962	350	307#	215	5177	On 300 - 500 m High Rise	M8	120	Clear
169	10°40.2'N	173°33.0'E	5407	300	233#	163	5570	Late Albian	...	100-104	Clear
170	11°48.0'N	177°37.0'E	5792	200	192#	134	5926	Late Albian	...	100-104	Clear
194	33°58.7'N	148°48.6'E	5744	400	256	280	6024	...	M17	137	Clear
195	32°46.4'N	146°58.7'E	5958	450	392	315	6273	...	M18-19	140	Clear
196	30°07.0'N	148°34.5'E	6184	400-750	377	525	6709	...	M22	148	Faint Reflector at 750 m on Aries 7 profile
197	30°17.4'N	147°40.5'E	6143	300	278#	195	6338	...	M23	150	Poor
199‡	13°30.8'N	156°10.3'E	6090	>300	465	350(est)	6440	In Trough Next to Large Guyot	...	...	Unclear
303	40°48.5'N	154°27.1'E	5609	300	285#	200	5809	Hauterivian	M4	117	Very clear
304	39°20.3'N	155°04.2'E	5630	300	335#	235	5865	Hauterivian	M9	121	Very clear
307	28°35.3'N	161°00.3'E	5696	350	297#	208	5904	Tithanian-Berriasian	M21	145	Clear

Data are from Fischer et al. [1971], Winterer et al. [1971, 1973], Heezen et al. [1973], and Larson et al. [1975].

*Assuming sediment velocity of 2 km/s and density of 1.7 g cm^{-3}. For these sediment thicknesses this generally overestimates the thickness and provides an upper limit on the loading effect.

†Based on lineations of Larson and Chase [1972] and Hilde et al. [1976], with time scale from Larson and Hilde [1975].

‡These sites have not been plotted in Figure 13.

#At these sites, basalt was drilled, and unless otherwise stated, the evidence was that this was basement. Penetration in these cases is to the top of the basalt.

sediment correction

$$\Delta d = t_s \frac{\left(\rho_m - \rho_s\right)}{\left(\rho_m - \rho_w\right)}$$

Δd - sediment correction

t_s - sediment thickness

ρ_s - sediment density

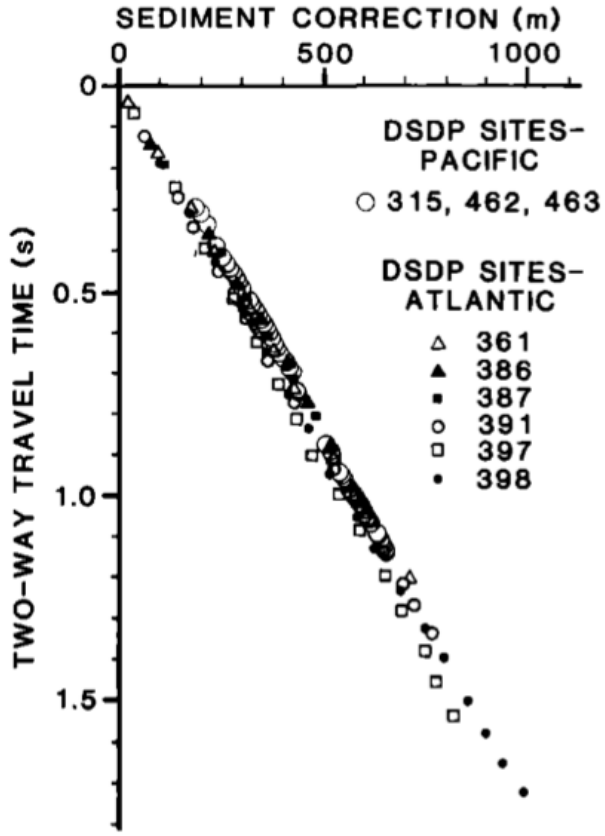

Fig. 9*a*. The empirical relatiohship of *Crough* [1983] between the standard mass balance sediment correction and the two-way travel time of seismic waves through the sediment column. Data from the North Pacific have been included. The linearity of this relationship is due to the self-cancellation of increases in velocity and density with depth.

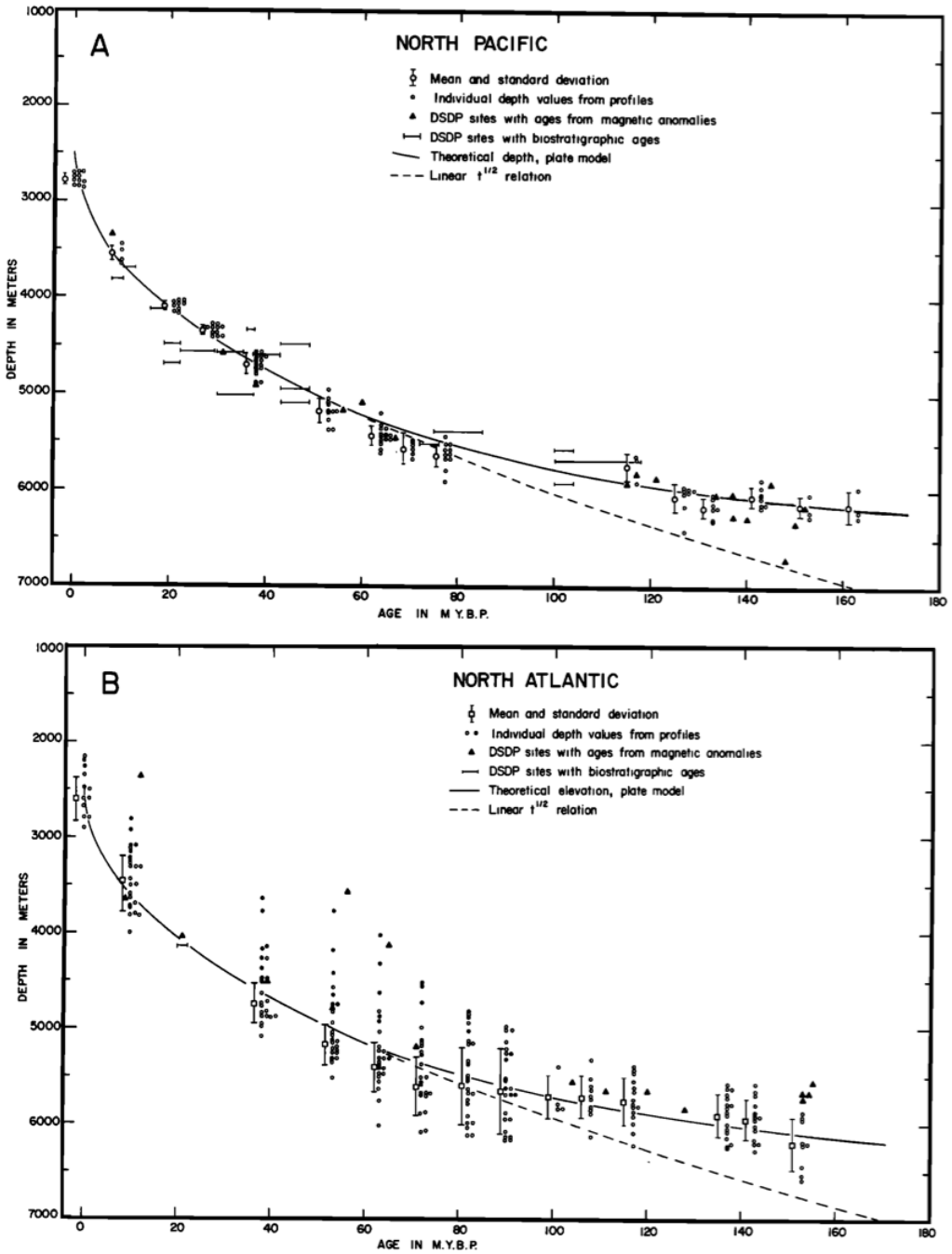

Fig. 13. Plot of individual depth measurements used in calculating mean depths and depths at DSDP sites for (a) the North Pacific and (b) the North Atlantic, illustrating the scatter in depths about the mean value. The means and standard deviations from the individual profile measurements are offset 2 m.y. The correct age is represented by the first column of individual points, some points being slightly offset for clarity. The solid circles in Figure 13b are points from profiles north of 31°N in the data set of Sclater et al. [1975].

model	T_m (C°)	α (10^{-5} C^{-1})	L (km)
P&S NA	1333+/-274	3.28+/-1.19	125+/-10
P&S PA	1365+/-276	3.1+/-1.11	128+/-10
GDH1	1450+/-250	3.1+/-0.8	95+/-15
CHABLIS	1340+/-30	4.2	112+/-7
H&W - best	1522+/-180	2.57+/-0.4	115+/-16
H&W –physical	1363	2.77	120

A model for the global variation in oceanic depth and heat flow with lithospheric age

Carol A. Stein* **& Seth Stein†**

* Department of Geological Sciences, University of Illinois at Chicago, Chicago, Illinois 60680, USA
† Department of Geological Sciences, Northwestern University, Evanston, Illinois 60208, USA

Variations in sea-floor depth and heat flow with age provide the main constraints on the thermal structure and evolution of the oceanic lithosphere. Joint fitting of heat flow and bathymetry yields a model with a hotter, thinner lithosphere than in previous models. The new model provides a significantly better fit to the data, including those from older lithosphere previously treated as anomalous. This will facilitate the analysis of lithospheric processes, including the effects of mid-plate volcanism and swells, regional subsidence, and hydrothermal circulation near spreading centres.

model	T_m (C°)	α (10^{-5} C^{-1})	L (km)	k (W m
P&S NA	1333+/-274	3.28+/-1.19	125+/-10	3.1
P&S PA	1365+/-276	3.1+/-1.11	128+/-10	3.1
GDH1	1450+/-250	3.1+/-0.8	95+/-15	3.25
CHABLIS	1340+/-30	4.2	112+/-7	4.2
H&W - best	1522+/-180	2.57+/-0.4	115+/-16	3.14
H&W –physical	1363	2.77	120	3.37

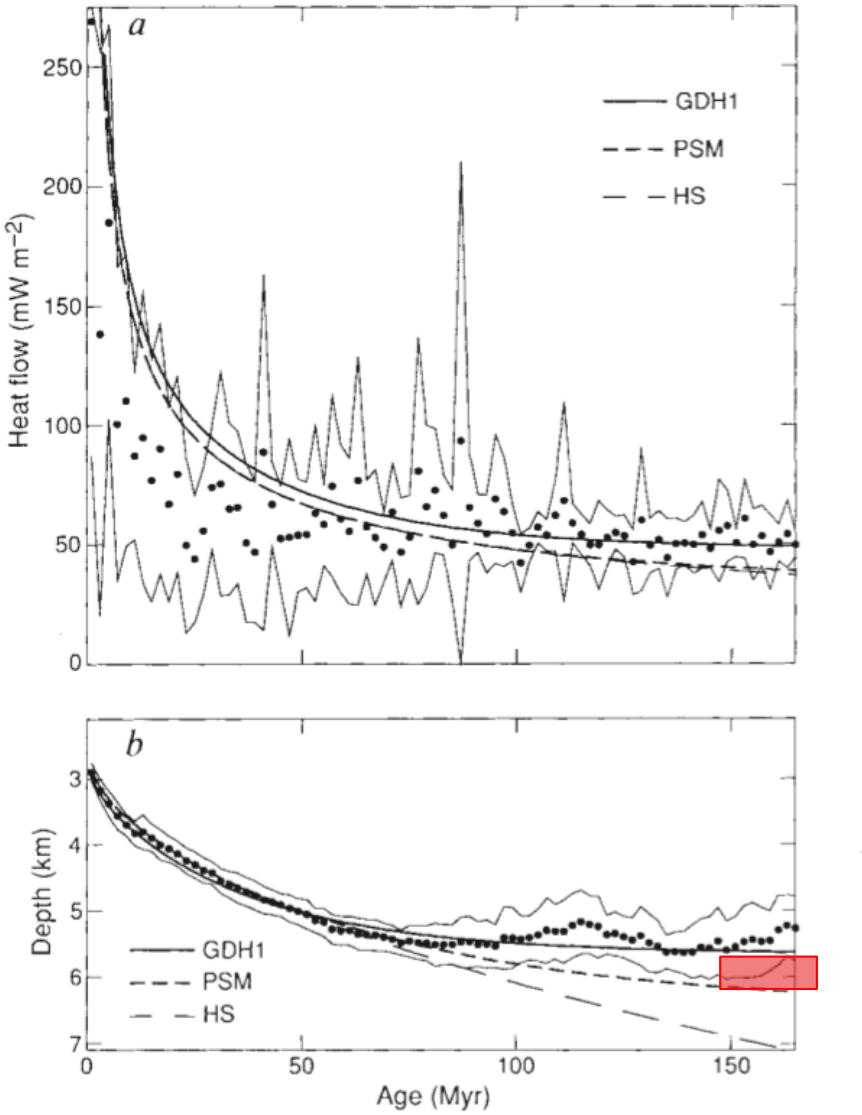

FIG. 1 Data and models for (*a*) heat flow and (*b*) ocean depth as a function of age. Depths are an average of North Pacific[24] (north of the Equator) and Northwest Atlantic[25] (15° N–45° N, 40° W–80° W) values: heat flow are from sites (Fig. 2) in these regions. The data are averaged in 2-Myr bins, and one standard deviation about the mean value for each is shown by the envelope. Shown are the plate model of Parsons and Sclater[12] (PSM), a cooling halfspace model with the same thermal parameters (HS) and the GDH1 plate model derived here. In *a*, the HS and PSM curves overlap for ages younger than ~120 Myr.

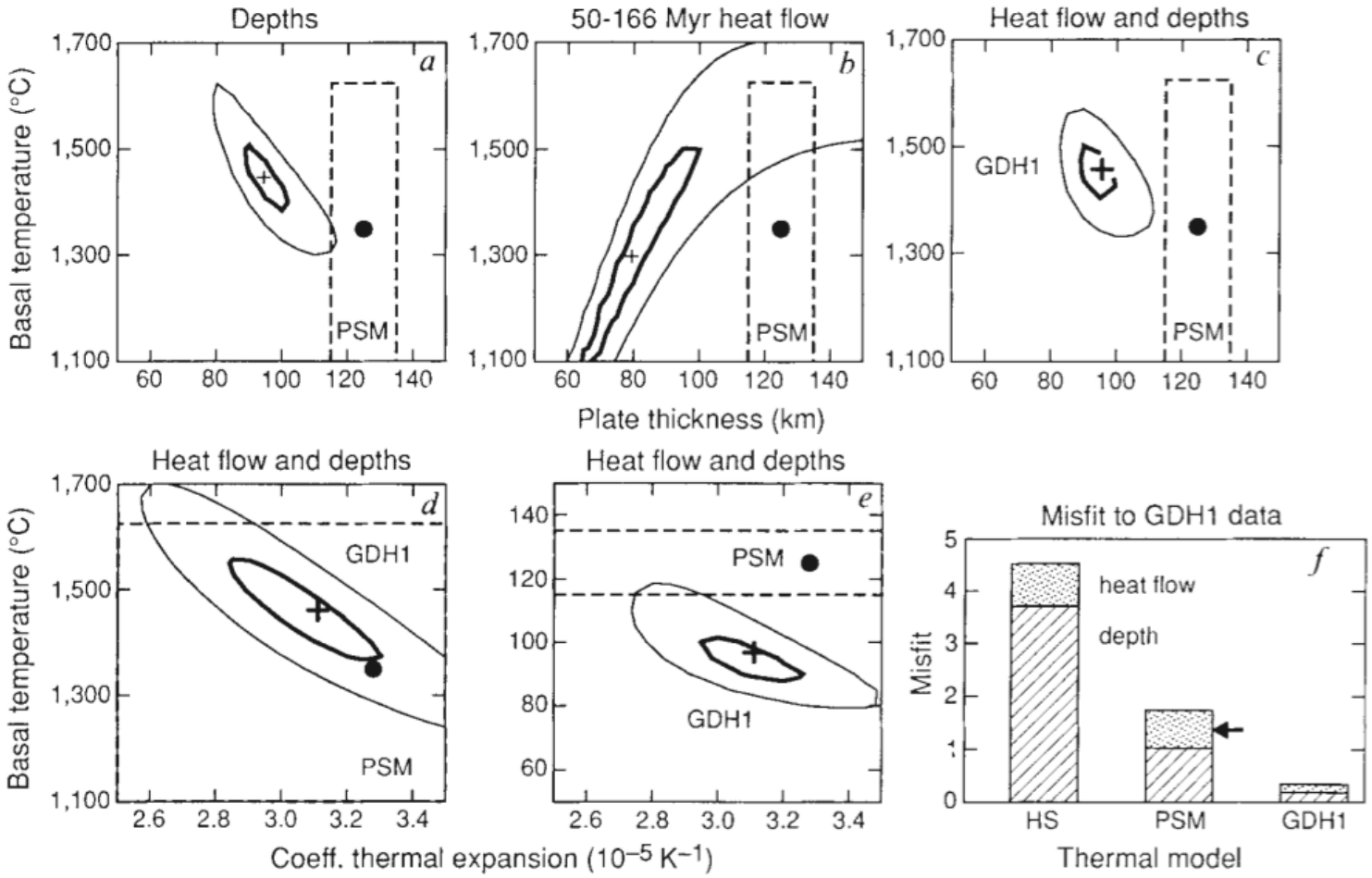

FIG. 3 *a–e*, Contour plots of the misfit to subsets of the data as a function of combinations of the three parameters. In each panel, the best fit is denoted by a cross, and the contours show values 1.25 and 2.5 times the minimum misfit. Parsons and Sclater's values (PSM) and their estimated uncertainties are also indicated. The best-fitting solution for the combined depth and heat flow (*c–e*), a 95-km-thick plate with a basal temperature of 1,450 °C and coefficient of thermal expansion $3.1 \times 10^{-5}\,K^{-1}$, is model GDH1. *f*, Misfit to the data for GDH1, PSM, the halfspace model and a version of the PSM model including radioactivity (arrow), which predicts the same depths but higher heat flow than PSM.

model	T_m (C°)	α (10^{-5} C^{-1})	L (km)	k (V
P&S NA	1333+/-274	3.28+/-1.19	125+/-10	3.1
P&S PA	1365+/-276	3.1+/-1.11	128+/-10	3.1
GDH1	1450+/-250	3.1+/-0.8	95+/-15	3.25
CHABLIS	1340+/-30	4.2	112+/-7	4.2
H&W - best	1522+/-180	2.57+/-0.4	115+/-16	3.14
H&W –physical	1363	2.77	120	3.37

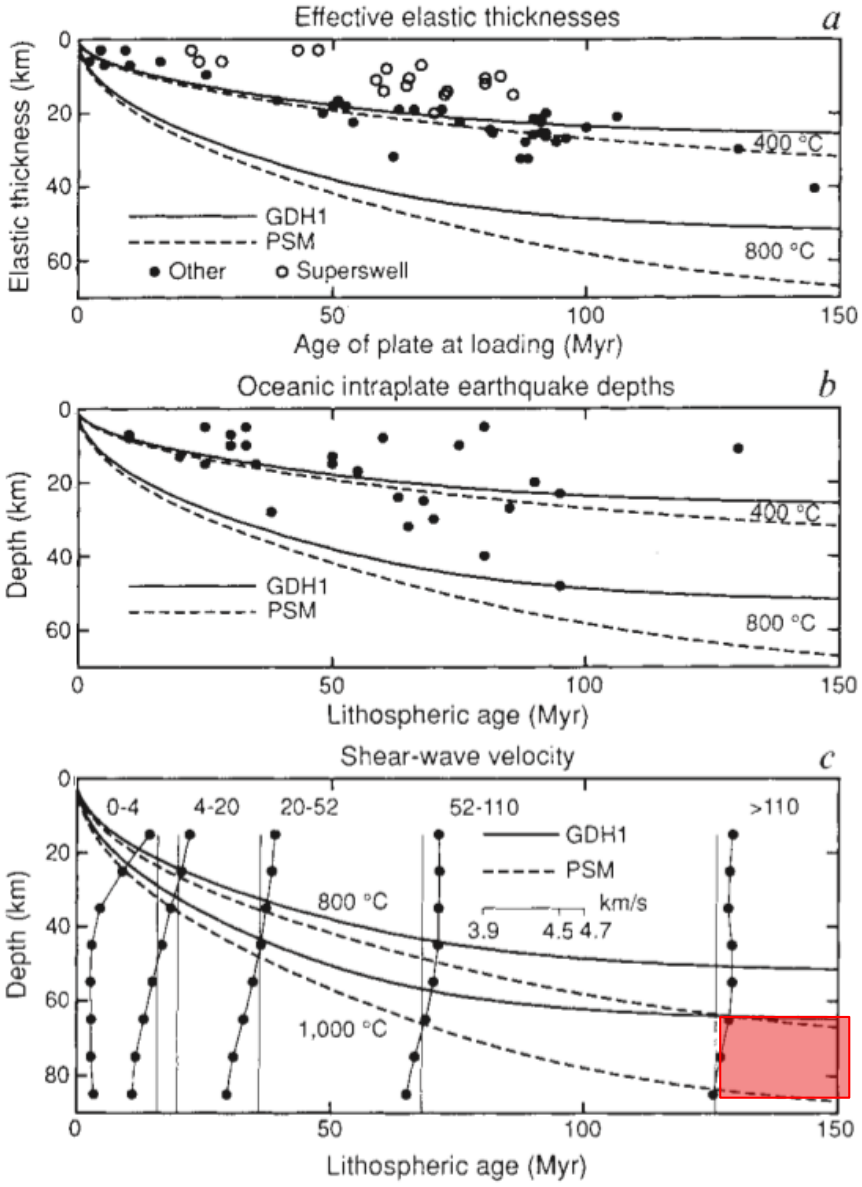

FIG. 6 Comparison of the isotherms as a function of age for the PSM and GDH1 models to three data sets[22,23,56] whose variation with age is consistent with cooling of the lithosphere. Except for the oldest lithosphere, the isotherms corresponding to the effective elastic thickness (*a*) and deepest intraplate seismicity (*b*) are similar for the two models. The difference between the temperatures for the low-velocity zone (*c*) is greater. The vertical line for the velocity structure in each age range (for example 0–4 Myr) corresponds to 4.5 km s^{-1}.

Thermal evolution of the oceanic lithosphere: an alternative view

M.P. Doin *, L. Fleitout

URA CNRS 1316, Laboratoire de Geologie, E.N.S. 24 rue Lhomond, 75005 Paris, France

Received 9 October 1995; accepted 23 April 1996

Abstract

The most common model used for representing the evolution with age of the oceanic lithosphere is the 'plate model' where the temperature is set at a fixed depth, called the base of the plate. This 'base of the plate' has no physical meaning but this model provides a mathematical substitute for a system where small-scale convection occurs through instabilities growing at the base of the cooling lithosphere and becomes effective only below old ocean. Another possible view is that convection provides heat at the base of the lithosphere whatever the age of the overlying plate. This last process can be modeled by a Constant Heat flow Applied on the Bottom Lithospheric ISotherm (CHABLIS model). A good fit to the observables (bathymetry and geoid as function of age, and old age heat-flow) can be obtained both for plate and CHABLIS models in spite of an experimentally determined thermal expansion coefficient much larger than assumed in previous plate models. These models have important consequences for several geodynamic processes. The plate, at an age of 100 Ma is only 80 km thick for both models: melting above a hot-spot can then occur in the garnet–spinel transition field without much plate thinning. In the plate model the subsidence is stopped at an age of about 80 Ma while, according to the CHABLIS model, several hundred meters of subsidence are expected after 100 Ma. Thus the two models predict quite a different long-term pattern of subsidence in the sedimentary basins. Finally, in the CHABLIS model, the global cooling of the mantle coming from cold material eroded by secondary convection at the base of the plates is considerably larger than in plate models: it amounts to 40%, the remaining 60% being due to the subduction process.

Keywords: lithosphere; oceanic crust; cooling; heat flow; thermal history

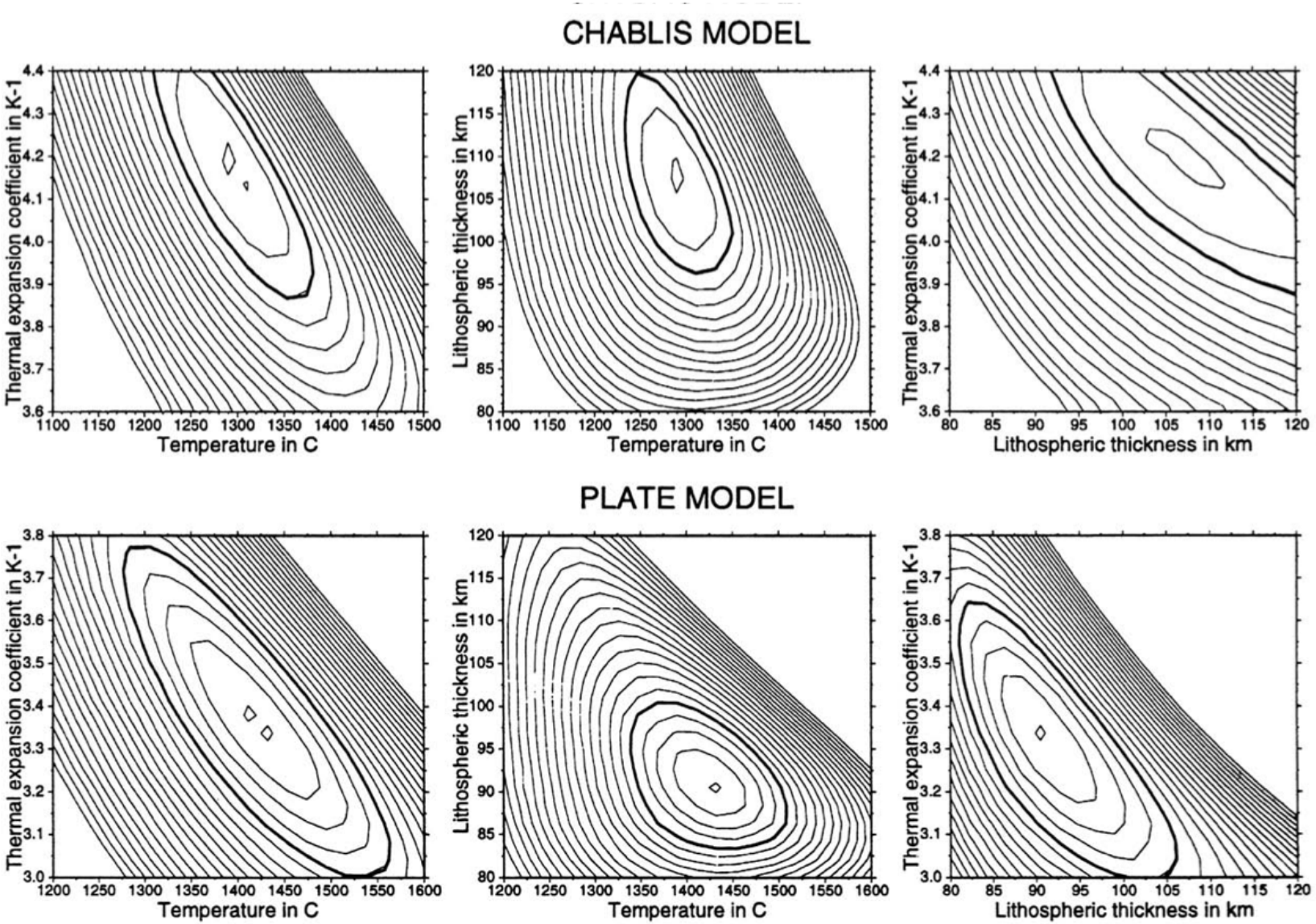

Fig. 2. Minimisation curves representing the function σ_t in planes passing through the minimum value. These curves correspond to inversion 1 of Table 3, both for the CHABLIS model (top) and the plate model (bottom). Fully temperature- and pressure-dependent parameters have been used in this inversion and the average thermal expansion coefficient is allowed to vary around the experimentally determined value. The average conductivity is fixed at 3.1 and the conductivity law $k_1(T)$ has been used. The spacing between isolines is 0.3. The thick line corresponds to the 1% confidence level for the parameters (F test).

model	T_m (C°)	α (10^{-5} C^{-1})	L (km)
P&S NA	1333+/-274	3.28+/-1.19	125+/-10
P&S PA	1365+/-276	3.1+/-1.11	128+/-10
GDH1	1450+/-250	3.1+/-0.8	95+/-15
CHABLIS	1340+/-30	4.2	112+/-7
H&W - best	1522+/-180	2.57+/-0.4	115+/-16
H&W –physical	1363	2.77	120

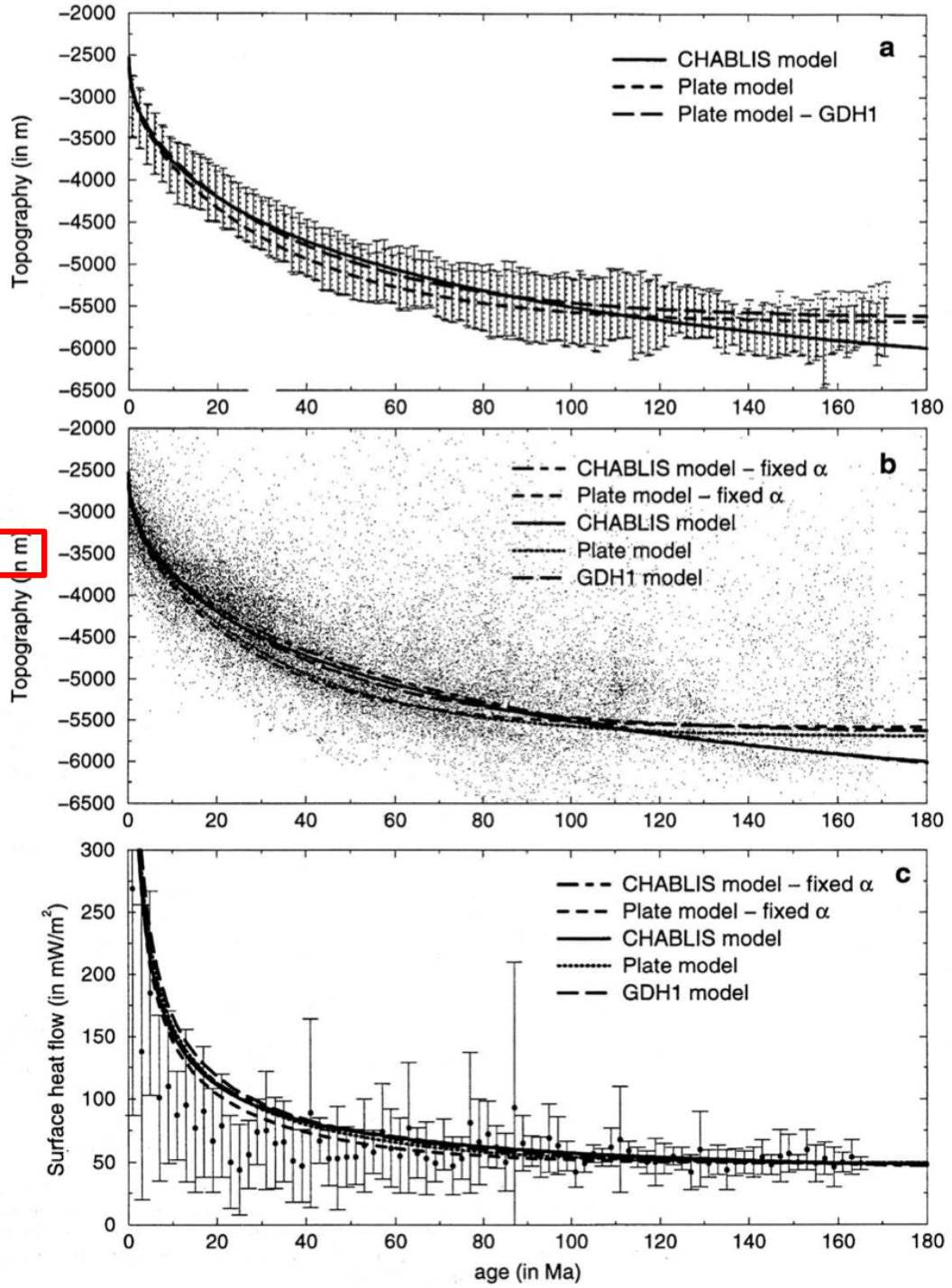

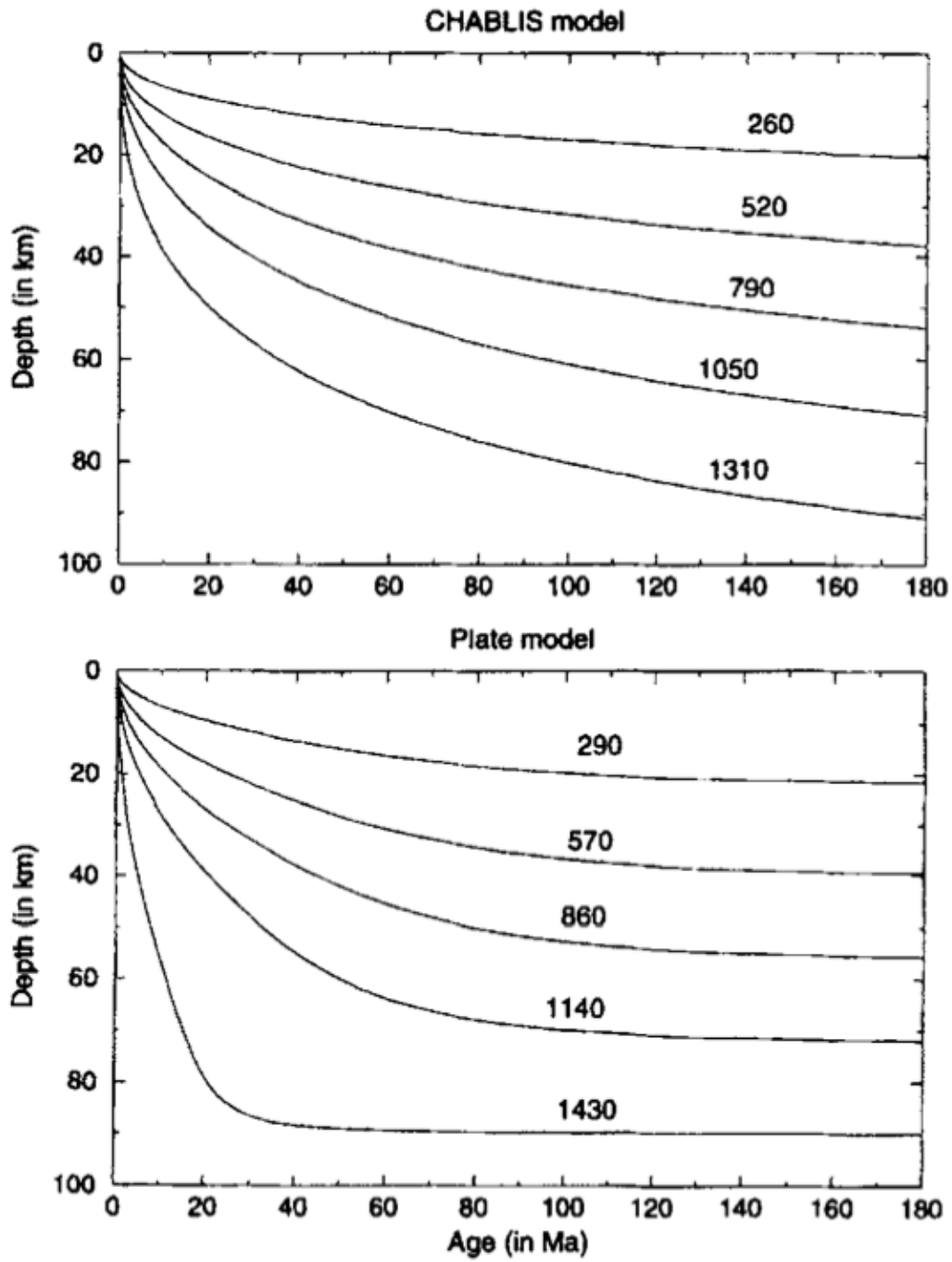

Fig. 6. Plate thickness and isotherms as function of age for the best-fit CHABLIS and plate models (inversion 1, Table 3).

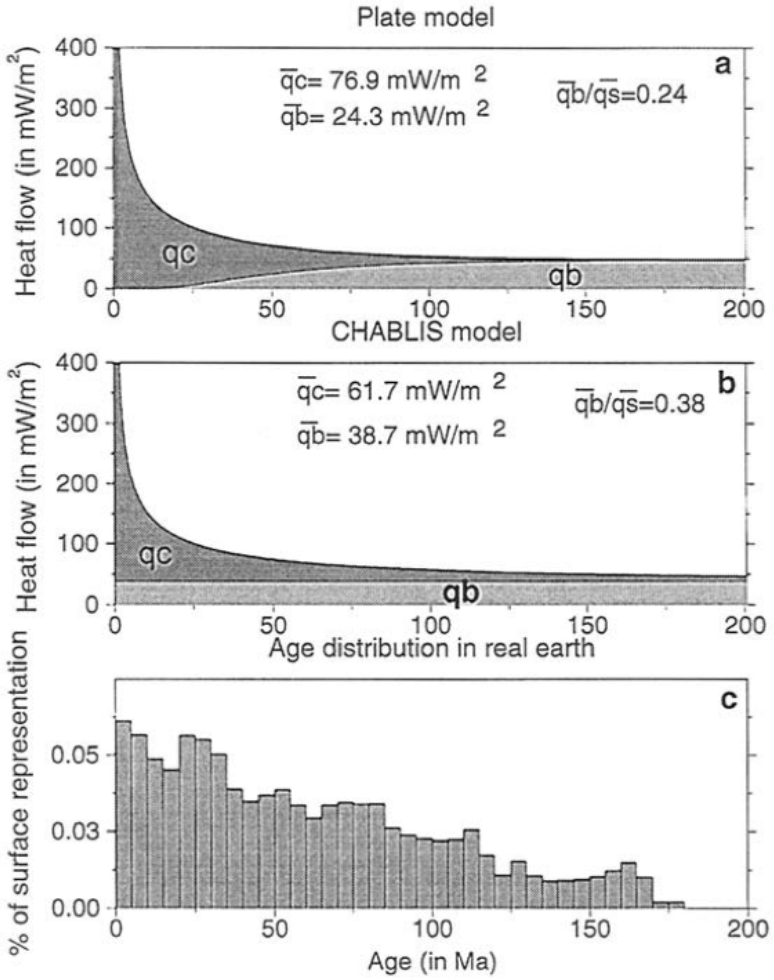

Fig. 7. Heat balance between primary and secondary convection. (a) The plate model. (b) The CHABLIS model. The upper curve (limit between dark grey and white) represents the surface heat-flow (q_s). The lower curve (limit between dark and light grey) represents the heat-flow at the base of the plate (q_b). The dark area represents the amount of coolness stored in the lithosphere per unit of time and area (q_c), while the light grey area represents the amount of coolness per unit of time and area transferred to the mantle by secondary convection (q_b). q_s represents the total amount of heat loss per unit of time and area. (c) The percent of the Earth's oceanic surface covered by plates of a given age range.

$$q_s = -\int_0^L \rho C_p \frac{\partial T}{\partial t} \mathrm{d}z + q_b = q_c + q_b$$

Relationship between depth and age in the North Pacific Ocean

J. K. Hillier and A. B. Watts

Department of Earth Science, University of Oxford, Oxford, UK

Received 25 August 2004; revised 22 November 2004; accepted 6 December 2004; published 24 February 2005.

[1] The North Pacific contains active mid-oceanic ridges and the oldest, Jurassic (166.8 ± 4 Ma), drilled oceanic crust. Its bathymetry is therefore critical to studies of the applicability of thermal contraction models (e.g., the infinite half-space and cooling plate) to the subsidence of seafloor with crustal age. The bathymetry, however, contains seamounts and oceanic islands (e.g., Mid-Pacific Mountains), oceanic plateaus (e.g., Hess, Magellan, and Shatsky), and midplate topographic swells (e.g., Hawaii), which are unrelated to the current plate-scale thermal state of the oceanic lithosphere. We use here a regional-residual separation algorithm called MiMIC to remove these features and to isolate the depths associated with the subsidence of North Pacific oceanic crust. These depths, z (m), increase with time, t (Ma), as $z = 3010 + 307\sqrt{t}$ until 85 Ma. For greater ages the depths "flatten" and asymptotically approach ~6.1 km and are well described by $z = 6120 - 3010 \exp(-0.026t)$. The flattening is not "abrupt" as recently described in z-t curves produced using the mean, median, and mode. As a result, the depths of both young and old seafloor are fit well (mean difference between and observed and calculated depths of 75 ± 54 m 1σ) by a single cooling plate model. Using a thermal conductivity, k, of 3.138 mW m^{-2} as previous studies, however, gives a plate of similar thickness (i.e., thermal thickness, L, of ~115 km) but one which is unreasonably hot (i.e., temperature at the base of the plate, T_b, of 1522 °C) and inexpansive (i.e., coefficient of thermal expansion, α, of 2.57×10^{-5} °C^{-1}). More reasonable values (i.e., $T_b = 1363$°C, $k = 3.371$ W m^{-1} °C^{-1}, $\alpha = 2.77 \times 10^{-5}$ °C^{-1}, and $L = 120$ km) are obtained if the crustal thickness is used to constrain T_b and a certain amount of the surface heat flow is allowed to be radiogenically generated within the oceanic lithosphere.

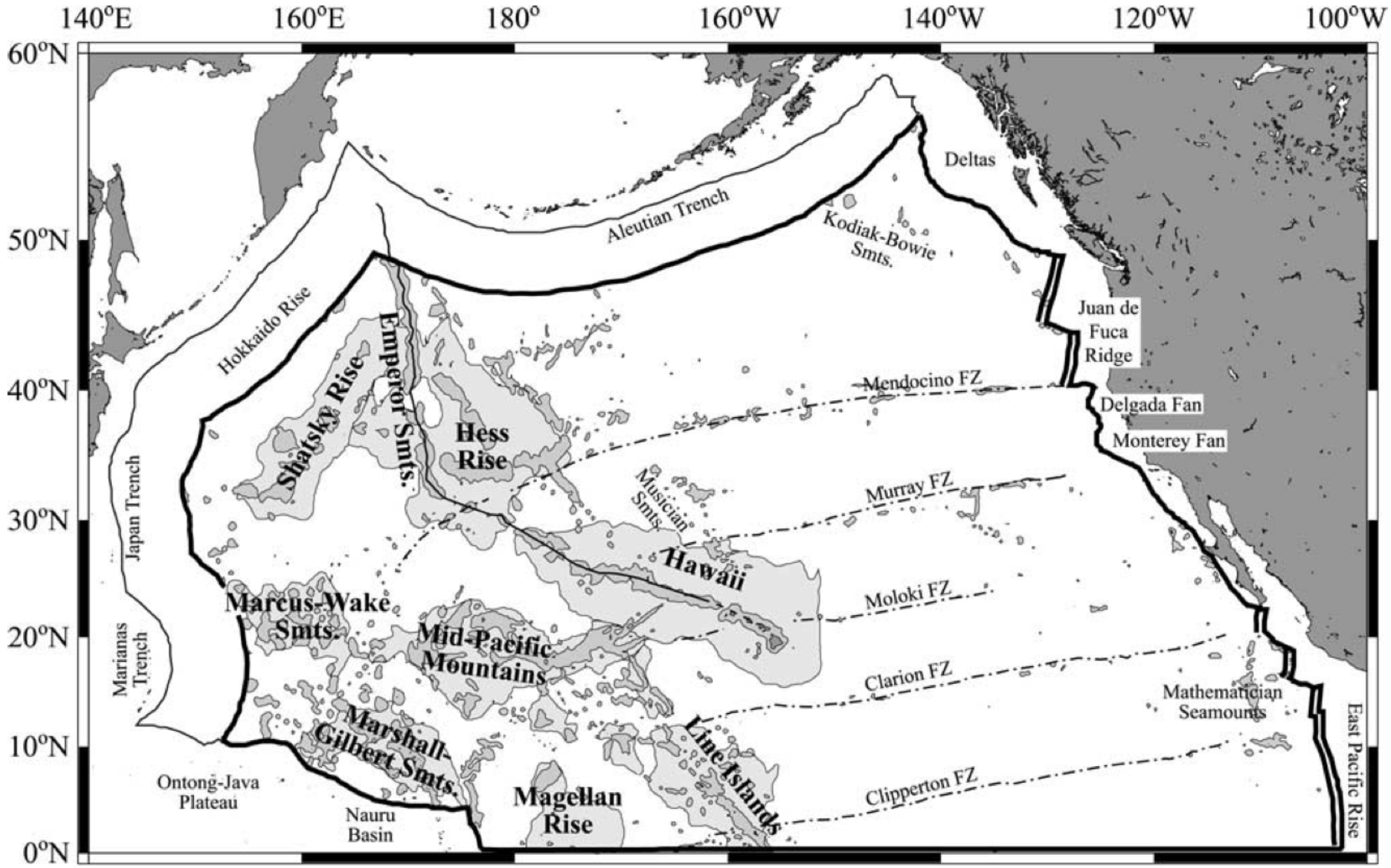

Figure 1. North Pacific. Dark gray shading is small-scale features such as seamounts based on the 500 m contour of the smoothed (50 km median) data from Figure 5a. Light gray shading is medium-scale features from Figure 5b. The area analyzed, surrounded by a bold outline, contains only the data that best represent the plate-scale subsidence of the seafloor (see text). Double parallel lines indicate active spreading. Fracture zones (FZ) are approximately located.

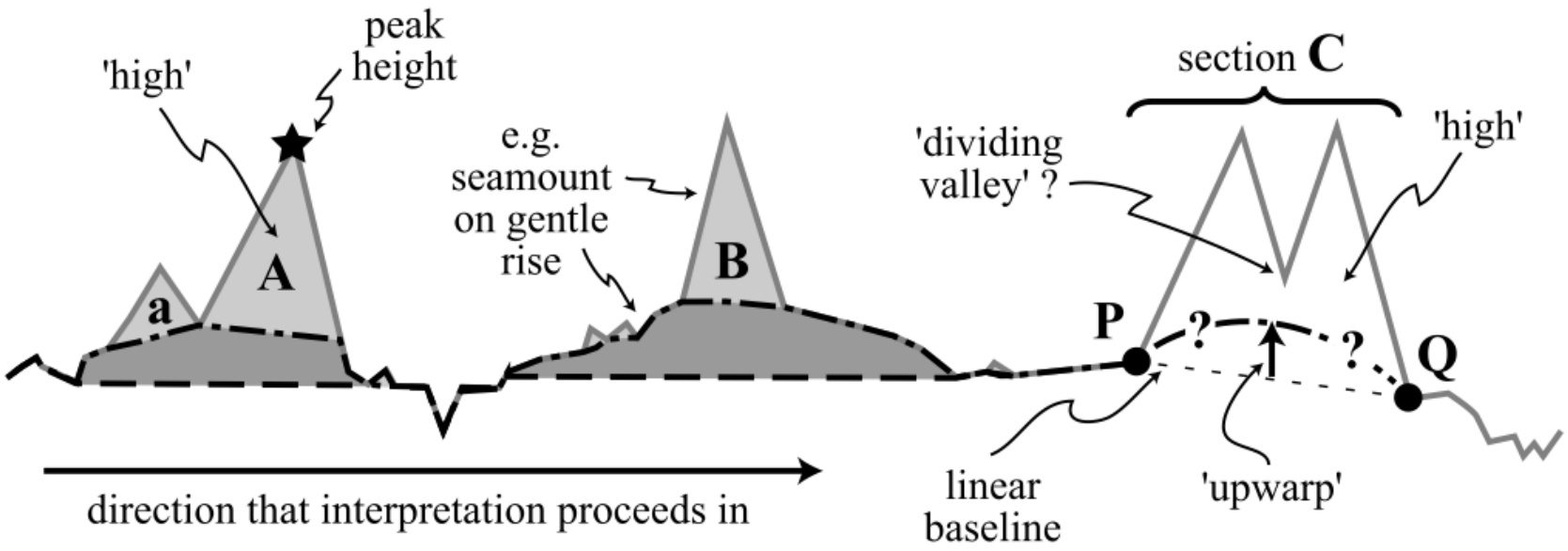

Figure 3. Illustration of the operation of MiMIC [*Hillier and Watts*, 2004] on a schematic bathymetric profile. See text for description. Solid dark gray line is bathymetry. Left of point P, dashed line is "regional" bathymetry (without small-scale bathymetric highs) deduced when the morphology of highs is not considered. Dot-dashed line is same but when morphology of highs is required to be "seamount-like" (i.e., for MiMIC set parameters $\bar{z}$, ϕ, and $\mathcal{U}$). Gray shadings (dark and light combined) are the highs "found" in the former case; light grays only (e.g., A, B, and a) are those found in the latter. A and a illustrate effect of restricting permissible peak height locations to center of sections (parameter ϕ). B is a seamount on a gentle rise and illustrates effect of restricting permissible range of $\bar{z}$. Section C illustrates $\mathcal{U}$, a quantification of the dilemma as to whether it is better to continue the interpretation directly between P and Q or to make the central dip a dividing valley.

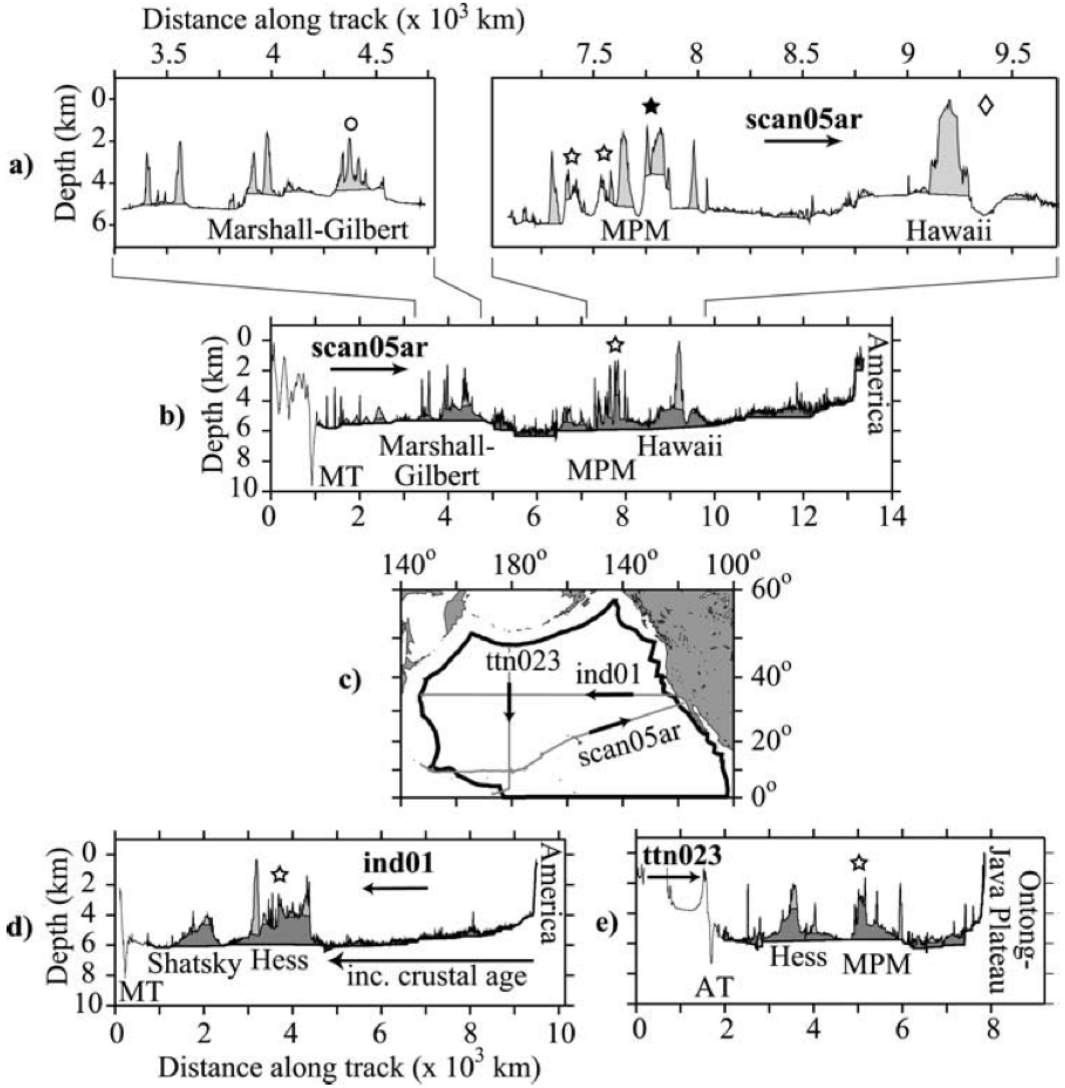

Figure 4. Operation of MiMIC along ship track profiles across the Pacific Basin. (a) Profile showing sections of bathymetry measured during cruise scan05ar. Top line is measured bathymetry, bottom line is bathymetry after the first application of MiMIC, and light gray shading is thus the small-scale bathymetric features isolated by this application. Stars highlight areas where the true interpretation is ambiguous and the regional of MiMIC may appear too shallow. Circle is where regional of MiMIC may be too deep. Diamond is where MiMIC follows seafloor down a flexural moat formed by seamount loading. (c) Map. Gray lines indicate track location, arrows are sailing direction, and bold outline is analysis area as in Figure 1. Cruises are 1976 cruise by research vessel (R/V) *Thomas Washington* NGDC 15040068 (ind01), 1969 cruise by R/V *Argo* NGDC 15010062 (scan05ar), and 1993 cruise by R/V *T. G. Thompson* NGDC 20010022 (ttn023). (b), (d), and (e) Full bathymetric profiles from cruises. Here results of a second application of MiMIC are also shown, and dark gray shading is the medium-scale features isolated. MPM, Mid-Pacific Mountains; MT, Marianas Trench; AT, Aleutian Trench.

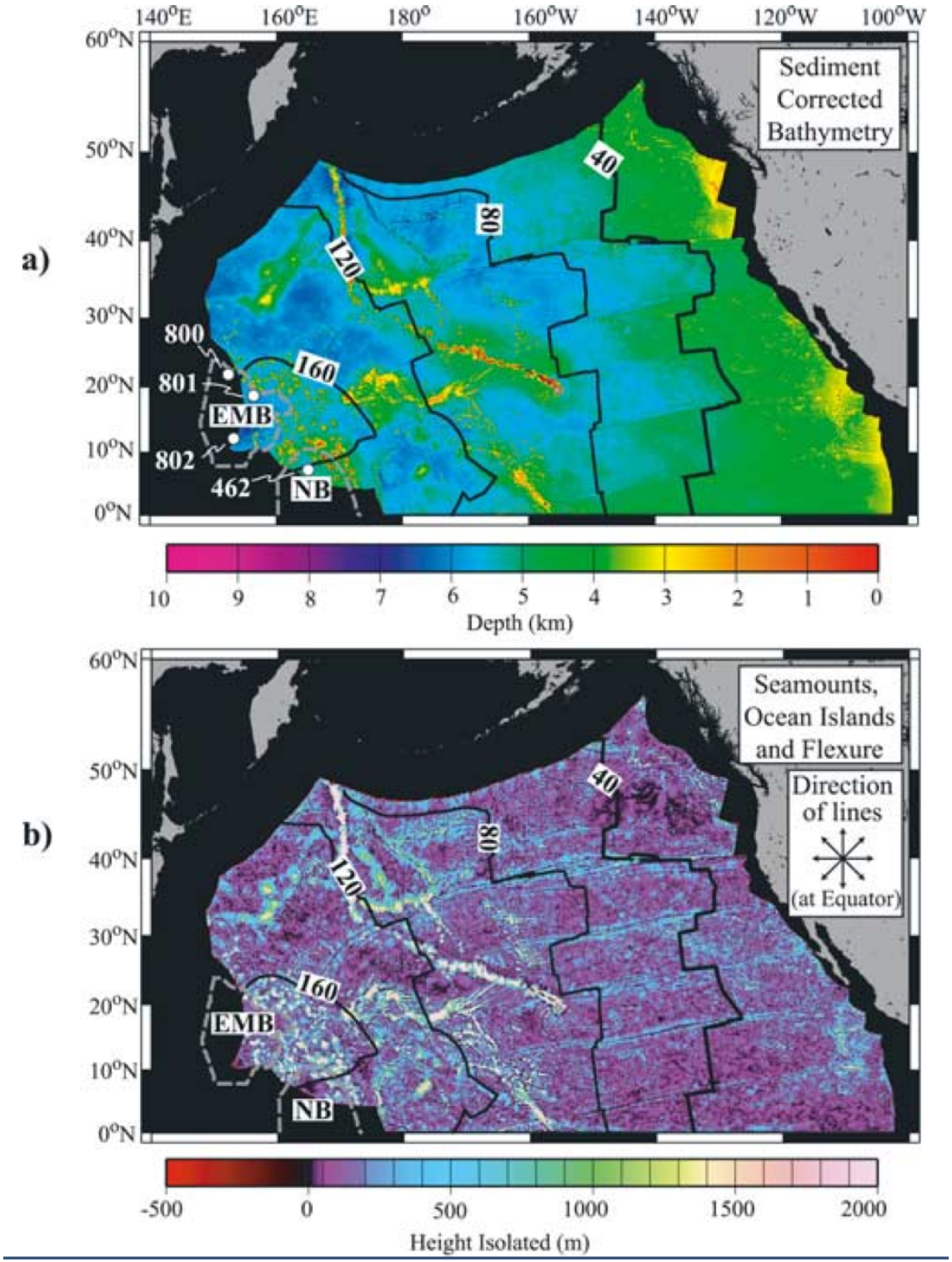
a)
140°E
160°E
180°
160°W
140°W
120°W
100°W
60°N
50°N
40°N
30°N
20°N
10°N
0°N
Sediment Corrected Bathymetry
40
80
120
160
800
801
EMB
802
462
NB
10
9
8
7
6
5
4
3
2
1
0
Depth (km)
b)
Seamounts, Ocean Islands and Flexure
Direction of lines
(at Equator)
-500
0
500
1000
1500
2000
Height Isolated (m)

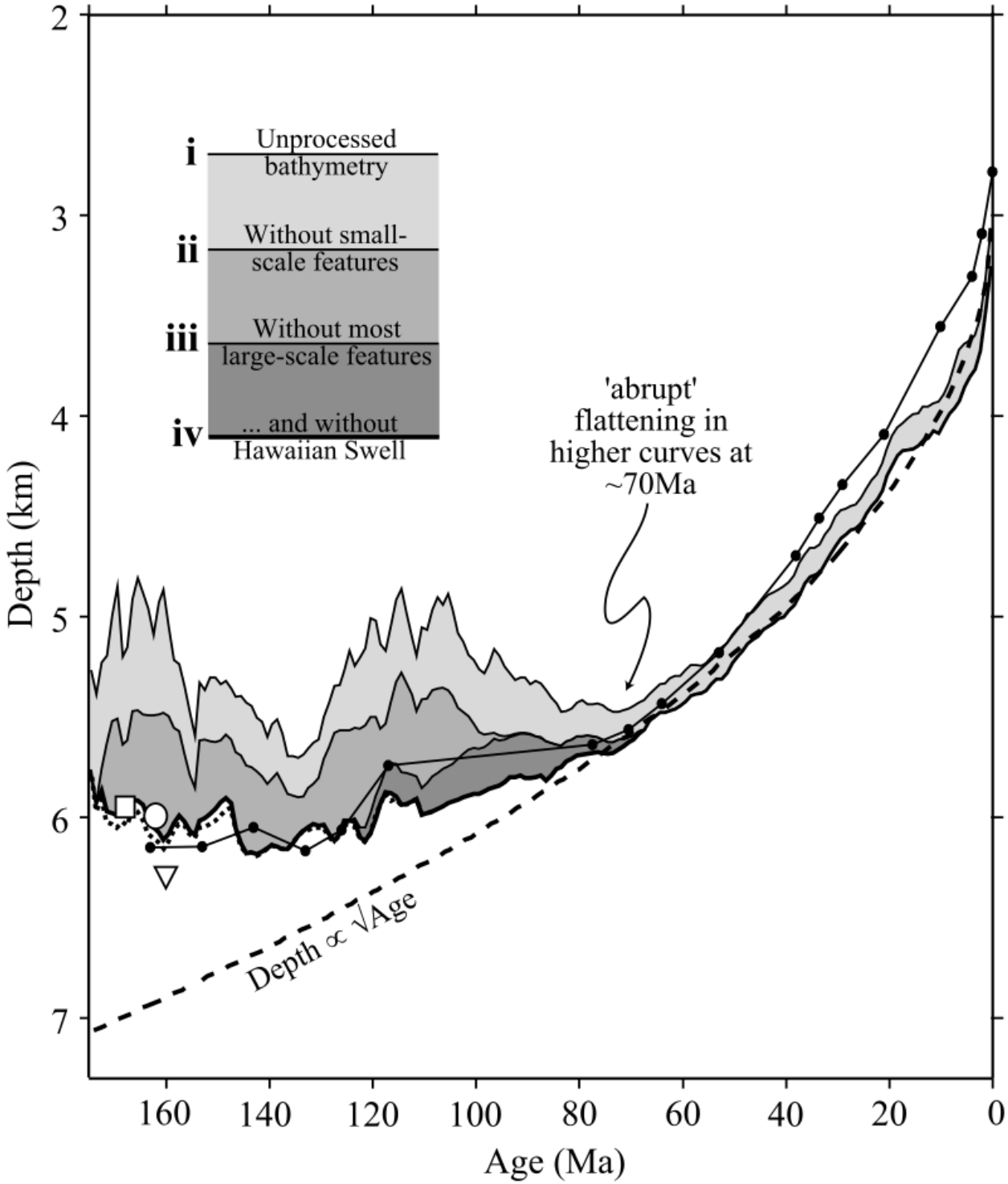
i
Unprocessed bathymetry
ii
Without small-scale features
iii
Without most large-scale features
iv
... and without Hawaiian Swell
'abrupt' flattening in higher curves at ~70Ma
Depth ∝ √Age
Depth (km)
Age (Ma)
2
3
4
5
6
7
160
140
120
100
80
60
40
20
0

6. Conclusions

[82] We draw the following conclusions from this analysis of bathymetry data in the North Pacific Ocean:

[83] 1. When small-scale (i.e., seamounts and oceanic islands) and medium-scale (i.e., oceanic plateaus and hot spot swells) bathymetric features are removed, North Pacific seafloor depths, z (m), are best approximated by subsidence proportional to the root of crustal age, t (Ma), for ages younger than 85 Ma. Depths then flatten asymptotically to ~6.1 km, about 1 km and greater than 2σ shallower than an extrapolation from young seafloor.

[88] 6. More reasonable material parameters for the model can be attained by constraining basal temperature by crustal thickness using geochemical relations to ~1350°C and allowing for some (4 mW m^{-2}) surface heat flow to be radiogenic in origin. These are T_b = 1363°C, k = 3.371 W m^{-1} $°C^{-1}$, $\alpha = 2.77 \pm 0.40 \times 10^{-5}$ $°C^{-1}$ and L = 120 km, although given the flexibility we have found in determining these parameters we are concerned about their literal interpretation.

Is crustal thickness uniform with age?

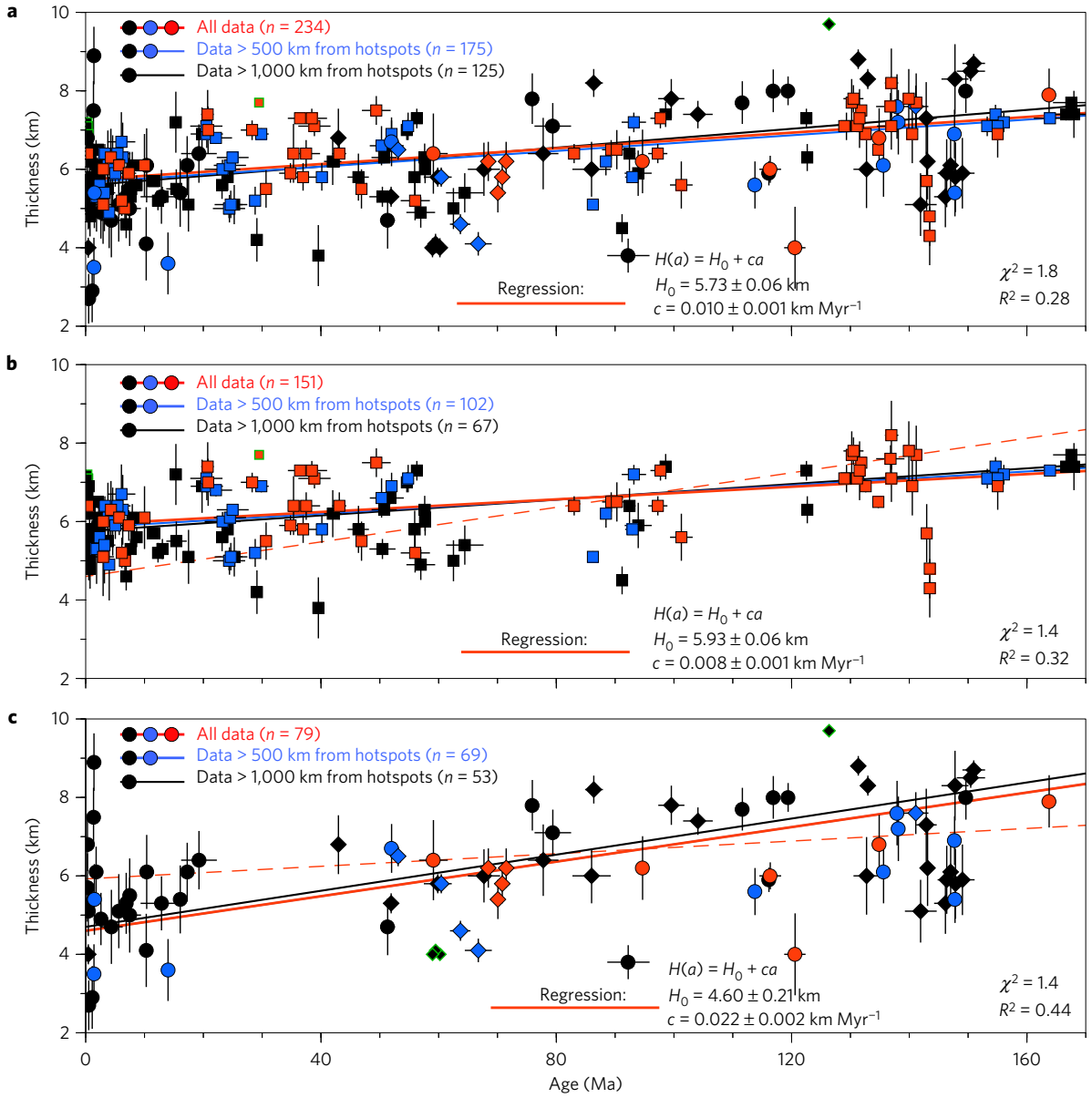

The estimated thickening of Pacific crust with age provides enough buoyancy to explain roughly **300m** of the observed flattening of seafloor depth as a function of plate age, an amount that is comparable to the seafloor depth misfit of current plate cooling models for the Pacific Ocean.

[Van Avendonk et al., 2016]

Figure 2 | Correlation between oceanic crustal thickness and plate age. a, Seismic crustal thickness data from all ocean basins (diamonds, Indian Ocean; squares, Pacific Ocean; circles, Atlantic Ocean). Outliers repressed in the linear regression have a green outline. **b**, Seismic data and linear regression for the Pacific Ocean basin alone. **c**, Seismic data and linear regression for the Atlantic and Indian Ocean basins. The red dashed line in **b**,**c** is added to compare the least-squares fit of the Pacific Ocean data and the Atlantic and Indian Ocean data.

Depth vs. Age – 28 years

- **Parsons and Sclater, 1977**
- **Stein and Stein, 1992**
- **Doin and Fleitout, 1996**
- **Hillier and Watts, 2005**

model	T_m (C°)	α (10^{-5} C^{-1})	L (km)	k (W m^{-1} C^{-1})
P&S NA	1333+/-274	3.28+/-1.19	125+/-10	3.1
P&S PA	1365+/-276	3.1+/-1.11	128+/-10	3.1
GDH1	1450+/-250	3.1+/-0.8	95+/-15	3.25
CHABLIS	1340+/-30	4.2	112+/-7	4.2
H&W - best	1522+/-180	2.57+/-0.4	115+/-16	3.14
H&W –physical	1363	2.77	120	3.37

Science 14 March 1997:
Vol. 275 no. 5306 p. 1613
DOI: 10.1126/science.275.5306.1613

PERSPECTIVE

Sea-Floor Depth and the Lake Wobegon Effect

Seth Stein, Carol A. Stein

± Author Affiliations

Geophysicists are directing renewed attention to the long-standing question of how to discriminate "normal" versus "anomalous" depths of portions of the oceans. The seemingly prosaic challenge of assessing whether depths deviating from an assumed norm are significant or simply artifacts of the reference model used (as in the mythical town of Lake Wobegon in the radio show Prairie Home Companion "where all children are above average") is surprisingly crucial to modern concepts of how the solid Earth functions. Put simply, sea-floor slopes and bumps provide much of our ideas about how Earth's heat engine operates and why it differs from those of neighboring planets.